

The ionisation and excitation state of stellar outflows

A. C. Raga, ICN, UNAM

June 18, 2007

1 Introduction

This course is meant as an introduction on how to include “microphysics” (i. e., the relevant physical and/or chemical processes) in dynamical calculations of HH jets. At the more basic level, this has to be done in order to have a more or less realistic calculation of the radiative cooling term, which is fundamental for obtaining a correct description of the dynamics of the gas. A more detailed description of the microphysics is necessary if one aims at obtaining predictions (e. g., emission line maps and line profiles) that can be compared directly with observations.

These notes cover the basics of how to introduce atomic microphysics in numerical models of outflows, covering from the most simple possible approach to the level of complexity necessary for obtaining predictions of the emission line spectrum. The introduction of chemical species is not directly discussed, but many of the considerations and methods described in these notes can be applied with only minor modifications to chemical networks.

2 The gasdynamic equations

The 3D, Cartesian equations of gas dynamics can be written in the following way :

continuity equation \rightarrow

$$\frac{\partial \rho}{\partial t} + \frac{\partial}{\partial x_j} \rho u_j = 0, \quad (1)$$

momentum equation (3 components) \rightarrow

$$\frac{\partial \rho u_i}{\partial t} + \frac{\partial}{\partial x_j} (\rho u_i u_j + P \delta_{ij}) = 0, \quad (2)$$

energy equation \rightarrow

$$\frac{\partial E}{\partial t} + \frac{\partial}{\partial x_j} [u_j (E + P)] = G - L, \quad (3)$$

with $E = \rho u_j u_j / 2 + P / (\gamma - 1)$ (γ is the specific heat ratio, $= 5/3$ for our discussion of a non-relativistic, atomic/ionic gas). In these equations, the implicit Einstein summation notation is used. We have used the standard notation: ρ = density, $u_i = i$ -th component of the flow velocity, $x_i = i$ -th spatial coordinate, t = time and P = pressure.

In an analogous way, one could write the MHD equations, which have extra terms due to the Lorentz force, and also include the vector induction equation (which describes the evolution of the magnetic field). The rest of the discussion in these notes mostly applies also to the MHD equations.

In the energy equation, we have the terms G and L , which are the thermal energy gain and loss (respectively) per unit volume and time. These two terms are the root of all microphysical evil.

Both of these terms depend on the atomic/ionic structure of the gas. There is both an energy gain and an energy loss associated with each of the species (for example, HI, HII, HeI, HeII, HeIII, CI, CII, CIII, ...) present in the gas, so that we have to compute them as :

$$G = \sum_a G_a; \quad L = \sum_a L_a, \quad (4)$$

where a is an index that numbers all of the species included in the model. In order to compute the G_a and L_a we need to know the value of the number densities n_a of all of the species. These number densities follow continuity equations of the form

$$\frac{\partial n_a}{\partial t} + \frac{\partial}{\partial x_j} n_a u_j = S_a, \quad (5)$$

where S_a is the source/sink term due to ionisations and recombinations (as well as charge exchange for some species). By combining equations (5) with equation (1) one can find the alternative set of equations

$$\frac{\partial y_a}{\partial t} + u_j \frac{\partial}{\partial x_j} y_a = \frac{S_a}{n}, \quad (6)$$

where $y_a = n_a/n$ is the fractional abundance of the species a (with $n = \rho/m$, m being the average mass per atom or ion).

Therefore, in order to solve the gasdynamic+microphysical problem one has to integrate the 5 gasdynamic equations (1)-(3) together with the set of equations for the ionisation network (equation 5, or alternatively equation 6). The network equations are coupled with the gasdynamic equations through the radiative energy gain and loss terms (see equation 4).

3 The ionisation state of the gas

3.1 The rate equations

For the sake of simplicity, in this section we consider the case of a constant density gas, for which the equations for an atomic/ionic network are :

$$\frac{dn_{a,z}}{dt} = S_{a,z}^c + S_{a,z}^{ph}, \quad (7)$$

with the collisional (S^c) and photoionisation (S^{ph}) source terms being given by

$$S_{a,z}^c = n_e [n_{a,z-1}c_{a,z-1} + n_{a,z+1}\alpha_{a,z+1} - n_{a,z}(c_{a,z} + \alpha_{a,z})], \quad (8)$$

$$S_{a,z}^{ph} = n_{a,z-1}\phi_{a,z-1} - n_{a,z}\phi_{a,z}. \quad (9)$$

If the $n_{a,z}$ are known, the electron density can be computed as

$$n_e = \sum_a \sum_z z n_{a,z}. \quad (10)$$

3.2 The collisional rate coefficients

The collisional ionisation (c) and radiative+dielectronic recombination (α) coefficients are functions of temperature T given by integrals of the form

$$\alpha(T), c(T) = \int_0^\infty f(v, T) \sigma_v v dv, \quad (11)$$

where $f(v, T)$ is the Maxwell-Boltzmann distribution for the electrons, and σ_v is the velocity-dependent collision cross section for the appropriate process.

It is common to give analytic fits to these coefficients in the ‘‘Arrhenius interpolation’’ form :

$$r(T) = b_1 T^{b_2} e^{b_3/T}. \quad (12)$$

As an example of other formulae, Aldrovandi & Péquignot (1973, 1976) have used an interpolation

$$r(T) = b_1 \left(\frac{T}{10^4} \right)^{-b_2} + b_3 T^{-3/2} \exp(-b_4/T) [1 + b_5 \exp(-b_6/T)] , \quad (13)$$

for recombination coefficients.

Then, the b_1, b_2, \dots coefficients are tabulated for all of the ionisation and recombination processes that have to be considered. An example of such a tabulation (taken from Raga et al. 2007) is given below.

Finally, we should note that for some atoms and ions, in the collision source term $S_{a,z}^c$ (see eq. 8) one also has to include “charge exchange” reactions with H. An example of important charge exchange reactions are the processes $\text{HII} + \text{OI} \rightarrow \text{HI} + \text{OII}$ and $\text{HI} + \text{OII} \rightarrow \text{HII} + \text{OI}$ (see table 1). These processes have rates of the form $n_{\text{HII}}n_{\text{OI}}q(T)$ and $n_{\text{HI}}n_{\text{OII}}q'(T)$, respectively, with the rate coefficients $q(T)$ and $q'(T)$ also given by Arrhenius interpolations (see table 1).

3.3 The photoionisation rates

The photoionisation rates are calculated as a function of the average intensity J_ν of the radiative field through the frequency integrals

$$\phi_{a,z} = \int_{\nu_{a,z}}^{\infty} \frac{4\pi J_\nu}{h\nu} \sigma_{a,z}(\nu) d\nu , \quad (14)$$

where ν is the frequency, $\nu_{a,z} = \chi_{a,z}/h$ is the frequency of the ionisation edge and $\sigma_{a,z}(\nu)$ is the photoionisation cross section. Here again, one can find tabulations of coefficients of power law interpolations for the $\sigma_{a,z}(\nu)$ (see, e. g., any of the versions of the book of Osterbrock).

The problem of course is that one has to solve a system of radiative transfer equations of the form

$$\frac{dI_\nu}{dl} = j_\nu - \kappa_\nu I_\nu \quad (15)$$

for the specific intensity I_ν (j_ν and κ_ν being the emission and absorption coefficients, respectively). This is a system of equations, since one has to solve this for many propagation directions (l being the distance element along a given direction) and frequencies.

Table 1: Ionisation, recombination and charge exchange coefficients

reaction	coefficients ^a
$e + \text{HI} \rightarrow 2e + \text{HII}$	1: 5.83×10^{-11} , 0.5, -157800
$e + \text{HII} \rightarrow \text{HI}$	1: 3.69×10^{-10} , -0.79, 0
$e + \text{HeI} \rightarrow 2e + \text{HeII}$	1: 2.707×10^{-11} , 0.5, -285400
$e + \text{HeII} \rightarrow \text{HeI}$	2: 4.3×10^{-13} , 0.672, 0.0019, 4.7×10^5 , 0.3, 94000
$e + \text{HeII} \rightarrow 2e + \text{HeIII}$	1: 5.711×10^{-12} , 0.5, -631000
$e + \text{HeIII} \rightarrow \text{HeII}$	1: 2.21×10^{-9} , -0.79, 0
$e + \text{CII} \rightarrow 2e + \text{CIII}$	1: 3.93×10^{-11} , 0.5, -283000
$e + \text{CIII} \rightarrow \text{CII}$	2: 3.2×10^{-12} , 0.770, 0.038, 9.1×10^4 , 2.0, 3.7×10^5
$e + \text{CIII} \rightarrow 2e + \text{CIV}$	1: 2.04×10^{-11} , 0.5, -555600
$e + \text{CIV} \rightarrow \text{CIII}$	2: 2.3×10^{-12} , 0.645, 7.03×10^{-3} , 1.5×10^5 , 0.5, 2.3×10^5
$e + \text{NI} \rightarrow 2e + \text{NII}$	1: 6.18×10^{-11} , 0.5 -168200
$e + \text{NII} \rightarrow \text{NI}$	2: 1.5×10^{-12} , 0.693, 0.0031 2.9×10^5 , 0.6, 1.7×10^5
$e + \text{NII} \rightarrow 2e + \text{NIII}$	1: 4.21×10^{-11} , 0.5, -343360
$e + \text{NIII} \rightarrow \text{NII}$	2: 4.4×10^{-12} , 0.675, 0.0075 2.6×10^5 , 0.7, 4.5×10^5
$e + \text{OI} \rightarrow 2e + \text{OII}$	1: 1.054×10^{-10} , 0.5, -157800
$e + \text{OII} \rightarrow \text{OI}$	2: 2.0×10^{-12} , 0.646, 0.0014 1.7×10^5 , 3.3, 5.8×10^4
$e + \text{OII} \rightarrow 2e + \text{OIII}$	1: 3.53×10^{-11} , 0.5, -407200
$e + \text{OIII} \rightarrow \text{OII}$	2: 3.1×10^{-13} , 0.678, 0.0014 1.7×10^5 , 2.5, 1.3×10^5
$e + \text{OIII} \rightarrow 2e + \text{OIV}$	1: 1.656×10^{-11} , 0.5, -636900
$e + \text{OIV} \rightarrow \text{OIII}$	2: 5.1×10^{-12} , 0.666, 0.0028 1.8×10^5 , 6.0, 91000
$e + \text{SII} \rightarrow 2e + \text{SIII}$	1: 7.12×10^{-11} , 0.5, -271440
$e + \text{SIII} \rightarrow \text{SII}$	2: 1.8×10^{-12} , 0.686, 0.0049 1.2×10^5 , 2.5, 88000
$\text{HI} + \text{NII} \rightarrow \text{HII} + \text{NI}$	1: 1.1×10^{-12} , 0, 0
$\text{HII} + \text{NI} \rightarrow \text{HI} + \text{NII}$	1: 4.95×10^{-12} , 0, -10440
$\text{HI} + \text{OII} \rightarrow \text{HII} + \text{OI}$	1: 2.0×10^{-9} , 0, 0
$\text{HII} + \text{OI} \rightarrow \text{HI} + \text{OII}$	1: 1.778×10^{-9} , 0, -220

^aThe interpolation formulae are of the form “1:” Arrhenius, or “2:” Aldrovandi & Péquignot (1973), see equations (12) and (13)

After integrating these radiative transfer equations, one can then carry out the appropriate angular average

$$J_\nu = \frac{1}{4\pi} \oint I_\nu d\Omega \quad (16)$$

in order to obtain the average intensity of the radiative field.

Even though it is common practice to include photoionisation processes in 1D shock models (a practice started by Raymond 1976), very little work has been done in multi-dimensional simulations. There is the sole paper of Raga et al. (1999) in which the “diffuse” ionising photon field (i. e., the ionising photons produced by the shocked flow itself) was considered in a 3D jet model, and there are a few papers in which an external ionising photon field was introduced (in order to model HH jets within HII regions, see, e. g., Raga & Reipurth 2004). The more detailed descriptions of how to introduce photoionisation in multi-D simulations have been given by Mellema et al. (1998, 2006).

However, for models of jets in neutral or molecular regions, the photoionisation processes are only of secondary importance, and are normally not included in the models. Basically, it is normally assumed that CII and SII do not recombine to their neutral states because of the presence of enough photons below the Lyman limit within the region, and the problem of photoionisation is left at this. In these lecture notes, the complex problem of photoionisation is abandoned here and now.

3.4 Coronal ionisation equilibrium

If the temperature is kept constant, the ionisation state of the gas evolves to the point where $S_{a,z} = 0$ for all i and z . This condition (see equation 8) gives a system of linear equations which are equivalent to the system :

$$n_{a,z} c_{a,z} = n_{a,z+1} \alpha_{a,z+1}. \quad (17)$$

As can be seen, this system gives ionisation fractions $y_{a,z} = n_{a,z}/n_a$ (where $n_a = \sum_z n_{a,z}$) which are exclusively a function of T . This result holds if charge exchange reactions are included. The resulting ionisation fractions $y_{a,z}^c(T)$ are called the “coronal ionisation equilibrium” ionisation state.

Clearly, if we have an ionisation fraction $y_{a,z} > y_{a,z}^c(T)$, $y_{a,z}$ will evolve to a lower value with time, and the reverse is true for $y_{a,z} < y_{a,z}^c(T)$.

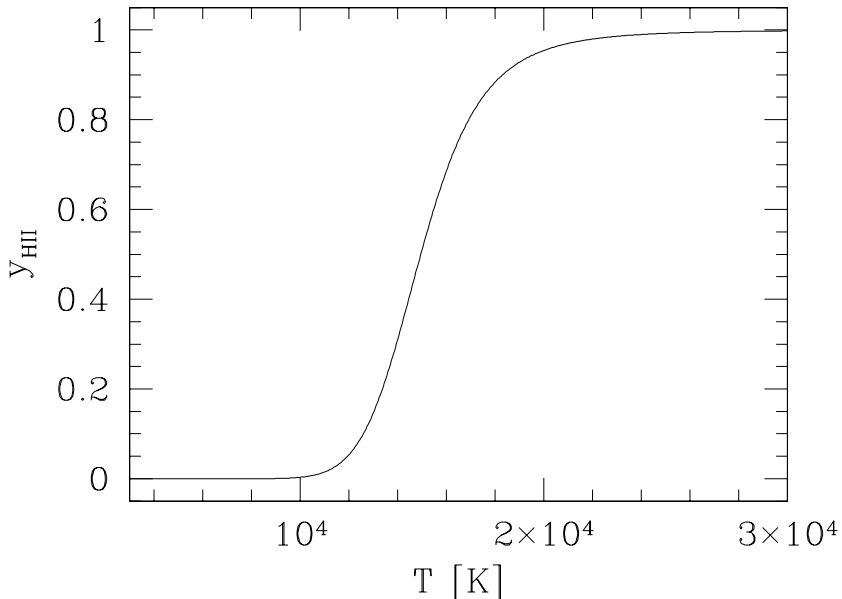


Figure 1: Coronal ionisation fraction of H as a function of temperature

As an example, let us consider the coronal ionisation equilibrium for H. Equation (17) is

$$n_{HI}c(T) = n_{HII}\alpha(T). \quad (18)$$

We can combine this equation with $n_H = n_{HI} + n_{HII}$ to obtain

$$y_{HII} = \frac{n_{HII}}{n_H} = \frac{1}{1 + \alpha(T)/c(T)}, \quad (19)$$

where the Arrhenius interpolations for the coefficients are $\alpha(T) = 3.69 \times 10^{-10}T^{-0.79}$ and $c(T) = 5.83 \times 10^{-11}T^{0.5} e^{-157800/T}$ (see equation 12 and the first two lines of table 1). The hydrogen ionisation fraction y_{HII} as a function of temperature T obtained from equation (19) is shown in Figure 1.

Life would be easy if the gas in shocked interstellar flows were in coronal ionisation equilibrium, as one could then make a tabulation of ionisation fractions as a function of temperature, and use this to obtain a tabulation of the cooling function as a function of density and temperature. However, the timescale for relaxation to coronal equilibrium is comparable to the cooling timescale of the flow, and therefore in many regions the ionisation state of the gas is well away from the coronal equilibrium state. Because of this, in order to obtain an accurate cooling function it is indeed necessary to integrate

continuity equations for all of the species relevant for the cooling term (see equation 5).

4 The cooling function

4.1 Introduction

In this section, we describe in some detail how to include the more important contributions to the cooling due to different processes. Actually, the cooling is dominated by collisional ionisation of HI and by collisional excitation of emission lines. We describe the radiative recombination and free-free losses only because it is very simple to include them, though they do not make an important contribution to the cooling function (at least for a gas with solar abundances).

4.2 Recombination and free-free cooling

When an electron passes by an ion and recombines, the kinetic energy of the electron is lost from the thermal energy reservoir. Analogously, when an electron loses kinetic energy in an inelastic collision (with the resulting emission of a photon), the thermal energy of the gas is reduced.

The free-free energy loss (per unit time and volume) due to the interaction of H ions and free electrons is given by :

$$L_{ff}(HII) = n_e n_{HII} \beta_{ff}(T), \quad (20)$$

where the interpolation formula

$$\beta_{ff}(z, T) = 1.846 \times 10^{-27} z^2 T^{1/2}, \quad (21)$$

can be used (see the book of Osterbrock). In this interpolation function, one has to set a charge $z = 1$ for HII. One can use the same function (i. e., with $z = 1$) for calculating the free-free losses due to He II ions (this of course being only an approximation because He I is not a hydrogenic ion) and the function with $z = 2$ for He III ions.

The radiative losses due to recombination of HII are given by :

$$L_{rec}(HII) = n_e n_{HII} \beta_{rec}(T), \quad (22)$$

where the interpolation formula

$$\beta_{rec}(t) = 1.133 \times 10^{-24} t^{-1/2} \left(-0.0713 + 0.5 \ln t + 0.640 t^{-1/3} \right) \quad (23)$$

with $t = 157890/T$ (see Seaton 1959). The contribution of the recombination of He ions can be computed with the scaling

$$\beta_{rec}(z, T) = z \beta_{rec}(1, T/z^2), \quad (24)$$

with $z = 1$ for HeII and $z = 2$ for HeIII.

4.3 Collisional ionisation

The energy loss due to collisional ionisation of the ion a, z can be written as

$$L_{a,z}^{ion} = n_e n_{a,z} c_{a,z}(T) \chi_{a,z}, \quad (25)$$

where $c_{a,z}(T)$ is the collisional ionisation coefficient and $\chi_{a,z}$ the ionisation potential of the ion a, z .

The terms that dominate the collisional ionisation cooling are the ionisation of HI, HeI and HeII. These terms dominate the cooling function for a neutral gas that is suddenly shocked to a temperature above a few times 10^4 K.

4.4 Collisionally excited lines

For each atom or ion that contributes substantially to the cooling function, one has to solve a system of equations giving the populations of the excited levels n_l ($l = 1, 2, \dots, N$ numbering in order of increasing energy all of the relevant levels) of the ion a, z . Of course, we have the relation

$$n_{a,z} = \sum_{l=1}^N n_l. \quad (26)$$

Once we have computed the n_l populations, we can compute the energy loss due to the collisional excitation of all of the relevant levels of the ion a, z as

$$L_{a,z}^{col} = \sum_{l=1}^N n_l \sum_{m<l} A_{l,m} h\nu_{l,m}, \quad (27)$$

where $A_{l,m}$ is the Einstein A coefficient for the spontaneous transition $l \rightarrow m$ and $h\nu_{l,m}$ is the energy associated with this transition.

The non-trivial problem of finding the populations n_l of the excited levels of course still remains. Because the relaxation time for the excitation/de-excitation of the levels is generally much shorter than the cooling and/or dynamical timescales of the flow, the calculation of the n_l is usually done under a statistical equilibrium assumption. The equilibrium condition results in the set of equations :

$$\sum_{m>l} n_m A_{m,l} + n_e \sum_{m \neq l} n_m q_{m,l}(T) = n_l \left[\sum_{m<l} A_{m,l} + n_e \sum_{m \neq l} q_{l,m}(T) \right], \quad (28)$$

where we have introduced the $q_{m,l}(T)$ which are the radiative excitation ($m < l$) or de-excitation ($m > l$) coefficients. For $m > l$, these coefficients are given by the expression

$$q_{m,l}(T) = \frac{8.629 \times 10^{-6} \Omega_{ml}(T)}{T^{1/2} g_m}, \quad (29)$$

where g_m is the statistical weight of the level at which the transition begins. The collisional excitation coefficients (i. e., $l \rightarrow m$ with $m > l$) are given by the relation

$$q_{l,m}(T) = \frac{g_m}{g_l} e^{-h\nu_{m,l}/kT} q_{m,l}(T). \quad (30)$$

The function $\Omega_{ml}(T)$ has a value of order 1, and is only slowly dependent on T . In many calculations, these ‘‘collision strengths’’ are considered to be constant, and taken from tabulations such as the classical one of Mendoza (1983). However, in our modern electronic world there is the database of the Arcetri/Cambridge/NRL ‘‘CHIANTI’’ atomic data base collaboration (<http://www.arcetri.astro.it/science/chianti/database/>) which has temperature-dependent interpolations of the collision strengths and the Einstein A coefficients of all of the transitions I have ever known.

We now proceed as follows. We assume that the A and q coefficients are known, as well as the temperature T (obtained, e. g., from a dynamical simulation) the electron density n_e and the ionic number density $n_{a,z}$ (both obtained from a solution of the non-equilibrium ionisation rate equations). We can then invert the system of linear equations (26) and (28) in order to find the populations n_l ($l = 1 \rightarrow N$) of the excited levels of the ion a, z .

Let us show how the equations look for a 3-level atom ($N = 3$). Equation (26) takes the form

$$n_1 + n_2 + n_3 = n_{a,z}. \quad (31)$$

Now, for $l = 1$, from equation (28) we obtain

$$n_1 [-n_e(q_{12} + q_{13})] + n_2(A_{21} + n_e q_{21}) + n_3(A_{31} + n_e q_{31}) = 0, \quad (32)$$

and for $l = 2$, we obtain :

$$n_1(n_e q_{12}) + n_2 [-A_{21} - n_e(q_{23} + q_{21})] + n_3(A_{32} + n_e q_{32}) = 0. \quad (33)$$

For $l = 3$, we obtain an equation that is a linear combination of equations (32-33).

Now, the system of 3 linear equations (31-33) can be inverted in order to find n_1 , n_2 and n_3 as a function of $n_{a,z}$, n_e and T .

4.5 The 2-level atom

Let us now consider a 2-level atom ($N = 2$). Equation (26) takes the form

$$n_{a,z} = n_1 + n_2, \quad (34)$$

and equation (28) takes the form

$$n_1 n_e q_{12} = n_2 (n_e q_{21} + A_{21}). \quad (35)$$

These two equations can be combined with equation (30) to obtain :

$$n_2 = \frac{n_{a,z}}{(g_1/g_2)e^{E_{21}/kT} + 1 + n_c/n_e}, \quad (36)$$

where the critical density is defined as $n_c \equiv A_{21}/q_{12}$. Then, for $n_e \ll n_c$ (the “low density regime”), we have

$$n_2 = \frac{n_{a,z} n_e q_{12}}{A_{21}}, \quad (37)$$

and for $n_e \gg n_c$ (the “high density regime”), we have

$$n_2 = \frac{n_{a,z} g_2 e^{-E_{21}/kT}}{g_1 + g_2 e^{-E_{21}/kT}}, \quad (38)$$

which is the Boltzmann distribution (LTE) population of level n_2 .

The energy loss associated with the transition between levels 2 and 1 is :

$$L_{21} = n_2 A_{21} h \nu_{21}, \quad (39)$$

which for the low density regime then takes the form

$$L_{21} = n_{a,z} n_e q_{12} h \nu_{21}, \quad (40)$$

and for the high density regime becomes

$$L_{21} = n_2(LTE) A_{21} h \nu_{21}, \quad (41)$$

These equations illustrate the well known fact that the collisionally excited line cooling function depends quadratically on the density for the “low density regime” and linearly for the “high density regime”.

5 Recipes for calculating the cooling function

5.1 Isochoric and coronal ionisation cooling functions

The most simple way to include a cooling function is to include in the energy equation (3) either the coronal ionisation equilibrium or the isochoric cooling.

The coronal ionisation equilibrium cooling is calculated as a function of density and temperature from the ionisation fractions calculated from the equilibrium equation (17). The cooling function is normally calculated for an atom+ion number density of 1 cm^{-3} , and the “user” scales it to higher (or lower) densities by assuming that it is in the “low density regime” (in which the cooling is proportional to the square of the density).

The isochoric cooling function is usually computed by considering a parcel with a time-independent density (of atoms+ions, usually of 1 cm^{-3}) which cools from a given initial temperature (typically 10^6 K). The non-equilibrium ionisation rate equations (7) are then integrated in time together with an energy equation of the form

$$\frac{3}{2} \frac{d}{dt} (n + n_e) kT = -L, \quad (42)$$

where n and n_e are the atom+ion and electron (respectively) number densities (n being time-independent, but not n_e). From the integration one obtains T and L as a function of time, and then one plots the radiative energy loss as a function of temperature in order to obtain the so-called “isochoric cooling function”.

The coronal equilibrium and isochoric cooling functions are tabulated in Table 2 (taken from De Colle 2007). These tables can be introduced in a code

Table 2: Coronal ionisation equilibrium and isochoric cooling functions

$\log_{10} T$ [K]	$\log_{10} L_{ce}$ [erg cm ⁻³ s ⁻¹] ^a	$\log_{10} L_{iso}$
3.9106	-26.0784	-25.5891
4.0006	-24.0161	-23.7582
4.0282	-23.5181	-22.8345
4.0601	-23.0615	-22.5186
4.0956	-22.6889	-22.3633
4.2008	-22.1165	-22.2669
4.4103	-22.0975	-22.2346
4.6313	-22.1336	-22.2015
4.7165	-22.0483	-22.1604
4.9465	-21.5183	-22.0718
5.1332	-21.2607	-21.7326
5.3338	-21.0870	-21.4906
5.4942	-21.0875	-21.2639
5.6010	-21.1587	-21.1075
5.7289	-21.2863	-21.0778
5.8089	-21.3616	-21.1810
5.9180	-21.4217	-21.3489
5.9809	-21.4289	-21.4227

^aThe coronal equilibrium and isochoric cooling functions are given for an atom+ion number density of 1 cm⁻³

(with an appropriate interpolation in $\log T$ in order to obtain a continuous function) and multiplied by the square of the number density of atoms+ions in order to obtain a cooling function to be used in the energy equation.

As far as I am aware, there are no publications yet describing the differences that are obtained in the dynamics of the flow when using one or the other of these cooling functions. Also, there is no discussion in the literature of how different are the resulting flow structures when one introduces a more accurate, many species non-equilibrium treatment of the ionisation and cooling.

5.2 Tabulations and interpolation functions

A detailed description of how to introduce an ionisation network with enough species so as to give a realistic cooling function is given by Raga, Mellema & Lundqvist (1997). These authors tabulate the cooling functions for a number of atoms and ions as a function of temperature and number density, and one can carry out an appropriate interpolation to obtain the numerical values of the cooling function for the desired densities and temperatures.

A reduced description of the cooling is proposed by Raga et al. (2002, 2007), who give a series of interpolation formulae which reproduce the low density regime of the ionic cooling functions of Raga et al. (1997). For example, the interpolations of the cooling due to the OI and OII ions are

$$\log_{10} \left(\frac{L_{OI}}{n_e n_{OI}} \right) = -45.0 + 1.23t_1 + 0.5t_1^{10} + 1.2t_2 + 1.2 [\max(t_2, 0)], \quad (43)$$

$$\log_{10} \left(\frac{L_{OII}}{n_e n_{OI}} \right) = -47.3 + 7.9t_3 + 1.9 \frac{t_4}{|t_4|^{0.5}}, \quad (44)$$

with $t_1 = 1 - 100/T$, $t_2 = 1 - 10^4/T$, $t_3 = 1 - 2000/T$, $t_4 = 1 - 5 \times 10^4/T$.

5.3 Cooling function including a single species ionisation network

A possibility first suggested by Hartigan & Raymond (1993) is to solve a single ionisation rate equation for HII (or for HI) and assume that $n_{OII}/n_O = n_{HII}/n_H$ (which approximately holds due to the similarity of the ionisation potentials of OI and HI, and the strong charge exchange reaction which couples O and H). Then, the cooling function can be computed including the collisional ionisation of H (see equation 25) and the cooling due to collisional excitation of O I and O II (equations 43-44).

Such a cooling function is appropriate only for temperatures below $\sim 2 \rightarrow 4 \times 10^4$ K. Therefore, one has to incorporate a switch to either the coronal or the isochoric cooling function for higher temperatures.

6 Calculation of the emitted spectrum

6.1 General considerations

Once we have calculated a dynamical model of an outflow (using a cooling function and an ionisation network such as the ones described above), we can proceed to compute the emission from the model flow. Typically, one wants to compute the emission in a set of lines which have been observed.

6.2 The emission coefficient

If we know the number density n_2 of the excited level which gives rise to a given transition $2 \rightarrow 1$, the total line emission coefficient can be computed as

$$j_{21}^{(L)} = \frac{n_2 A_{21} h \nu_{21}}{4\pi}. \quad (45)$$

The emission coefficient as a function of frequency ν is

$$j_{21}(\nu) = \frac{j_{21}^{(L)}}{\sqrt{\pi} \Delta \nu_D} e^{-(\nu - \nu_{21})^2 / \Delta \nu_D^2}, \quad (46)$$

where $\Delta \nu_D = \nu_{21} v_T / c$ with $v_T = \sqrt{2kT/m_a}$ (m_a being the mass of the element which gives rise to the line). Using the standard Doppler effect, one can obtain the emission coefficient as a function of radial velocity v_r (along the line of sight) :

$$j_{21}(v_r) = \frac{j_{21}^{(L)}}{\sqrt{\pi} v_T} e^{-v_r^2 / v_T^2}. \quad (47)$$

6.3 Optically thin lines

For an optically thin emission line, one can obtain an emission map by integrating $j_{21}^{(L)}$ (see equation 45) along lines of sight :

$$I_{21}(x, y) = \int j_{21}^{(L)}(x, y, z) dz, \quad (48)$$

where (x, y) are the plane of the sky coordinates, and z lies along the line of sight. In order to compare the predicted emission map with an observed map, a convolution with a simulated “seeing profile” or “point spread function” might be necessary.

Also, maps at a given radial velocity can be computed by integrating along lines of sight the radial velocity profile (equation 47) of the line :

$$I_{21}(v_r, x, y) = \int j_{21}(v_r - v^{(f)}_r, x, y, z) dz, \quad (49)$$

where $v^{(f)}_r(x, y, z)$ is the component along the line of sight of the velocity of the flow at position (x, y, z) .

From equation (49), one can compute line profiles at a given position (x, y) on the plane of the sky. In order to compare with an observation, a convolution with the spectral response function of the spectrograph might be necessary, as well as a plane-of-the-sky spatial integration or convolution in order to simulate the effect of the seeing and of the width (and/or length) of the spectrograph slit.

Also, one can carry out an integration of (49) over given radial velocity bins in order to obtain “radial velocity channel maps” that can be directly compared with Fabry-Pérot or with 2D field spectroscopic observations (again, a convolution with a “seeing function” might be appropriate).

6.4 Optically thick lines

For an optically thick line, one has to first calculate the optical depth to the position z along the line of sight :

$$\tau_{21}(v_r, x, y, z) = \int_{-\infty}^z \kappa_{21}(v_r - v^{(f)}_r, x, y, z') dz', \quad (50)$$

where κ_{21} is the absorption coefficient :

$$\kappa_{21}(v_r, x, y, z) = n_2(x, y, z) \left(\frac{g_2}{g_1} \right) \frac{c^2 A_{21}}{8\pi^{3/2} \nu_{21}^2 v_T} e^{(-v_r/v_T)^2}, \quad (51)$$

where c is the velocity of light, and v_T is the spatially dependent thermal velocity (see the text following equation 46).

The emission line map at a given radial velocity v_r can then be calculated as :

$$I_{21}(v_r, x, y) = \int j_{21}(v_r - v^{(f)}_r, x, y, z) \exp[-\tau_{21}(v_r, x, y, z)] dz. \quad (52)$$

This is the kind of treatment necessary to calculate the P-Cygni profiles which are obtained for stellar winds.

Somewhat more simple is the inclusion of the effect of dust extinction, because in this case the absorption coefficient has no radial velocity dependence (being approximately constant across the width of an emission line).

7 Summary

When one computes models of stellar outflows, one has to include a cooling function. This can be done in several different degrees of approximation :

- using a tabulated coronal ionisation equilibrium or isochoric cooling function (§5.1),
- including one extra continuity equation for HI or for HII (§5.3),
- including several atoms/ions (§5.2).

These three approaches give cooling functions which differ from each other by relatively large factors, and the effect of using the more simplified cooling functions should be evaluated quantitatively for the flow which one wants to simulate.

In order to obtain a prediction of the emitted spectrum, one has to have a prediction of the ionisation state of the gas. This can again be done by taking the coronal equilibrium or isochoric ionisation fractions (which would be consistent for a model calculated with the corresponding cooling functions), or by using the non-equilibrium ionisation state which is obtained from a full gasdynamic+ionisation network simulation.

One then has to compute the populations of the excited levels giving rise to the lines of interest, and compute the corresponding emission coefficients (§6.2). In this course we have given the details of how to compute the populations of levels excited by collisions (§4.4), but we have not given a description of how to do this calculation for levels populated by a recombination cascade (this can be found, e. g., in the book of Osterbrock 1989). This latter case of course applies for the H Balmer lines. With the emission line coefficients one can then carry out predictions of intensity maps, line profiles and radial velocity channel maps (§6.3) which can be compared directly with observations.

References

- [1] Aldrovandi, S. M. V., Péquignot, D. 1973, *A&A*, 25, 137
- [2] Aldrovandi, S. M. V., Péquignot, D. 1976, *A&A*, 47, 321
- [3] De Colle, F. 2007, private communication

- [4] Hartigan, P., Raymond, J. C. 1993, *ApJ*, 409, 705
- [5] Mellema, G., Iliev, I. T., Alvarez, M. A., Shapiro, P. R. 2006, *NewA*, 11, 374
- [6] Mellema, G., Raga, A. C., Cantó, J., Lundqvist, P., Balick, B., Steffen, W., Noriega-Crespo, A. 1988, *A&A*, 331, 335
- [7] Mendoza, C. 1983, in *Planetary nebulae (A83-49126 24-89)* (Dordrecht: Reidel), p. 143
- [8] Osterbrock, D. E. 1989, “Astrophysics of gaseous nebulae and active galactic nuclei” (Mill Valley: Univ. Sci. Books)
- [9] Raga, A. C., De Colle, F., Kajdič, P., Esquivel, A., Cantó, J. 2007, *A&A*, 465, 879
- [10] Raga, A. C., Reipurth, B. 2004, *RMxAA*, 40, 15
- [11] Raga, A. C., de Gouveia dal Pino, E. M., Noriega-Crespo, A., Mininni, P., Velázquez, P. F. 2002, *A&A*, 392, 267
- [12] Raga, A. C., Mellema, G., Arthur, S. J., Binette, L., Ferruit, P., Steffen, W. 1999, *RMxAA*, 35, 123
- [13] Raga, A. C., Mellema, G., Lundqvist, P. 1997, *ApJS*, 109, 517
- [14] Raymond, J. C. 1979, *ApJS*, 39, 1
- [15] Seaton, M. J. 1959, *MNRAS*, 119, 81